New BIOTECHNOLOGY 80 (2024) 37–45

Contents lists available at ScienceDirect

New BIOTECHNOLOGY

journal homepage: www.elsevier.com/locate/nbt

From food waste to eco-friendly functionalized polymer composites: Investigation of orange peels as active filler

Elia Pagliarini [a,1], Carmen Minichiello [b,1], Laura Sisti [b,*], Grazia Totaro [c], Loredana Baffoni [a], Diana Di Gioia [a], Andrea Saccani [b]

[a] Dipartimento di Scienze e Tecnologie Agro-Alimentari, Università di Bologna, Via Fanin 40, Bologna, Italy
[b] Dipartimento di Ingegneria Civile, Chimica, Ambientale e dei Materiali, Università di Bologna, Via Terracini 28, 40131 Bologna, Italy
[c] Dipartimento di Chimica e Chimica Industriale, Università di Pisa, Via G. Moruzzi 13, 56124 Pisa, Italy

ARTICLE INFO

Keywords:
Biocomposites
Food wastes
Orange peels
Poly(butylene succinate-co-adipate)
Antibacterial properties

ABSTRACT

The development of eco-friendly polymer composites with multifunctional properties aligns with the goals of the circular economy agenda, which aims to minimize waste and promote the sustainable use of resources by closing the loop of product life cycles. Eco-friendly polymer composites play a crucial role in achieving these objectives. The present work focuses on the preparation of fully biobased blends obtained by melt mixing a bio-polyester, poly(butylene succinate-*co*-adipate) (PBSA), with orange peels up to 20 wt%, to yield active polymer composites. Orange peels, employed here as natural filler, are largely available from food wastes, they are rich in phenolic compounds and possess antioxidant activity as shown by the experimental tests carried out. The thermal stability of the formulated composites is almost unchanged by the filler addition, showing only a slight decrease of the crystallization temperatures and crystalline fraction within the composites. The mechanical properties of the compounds evidence an increase in the elastic modulus together with a decrease in the tensile strength, while the elongation at break remains almost constant. The incorporation of the natural filler enabled the integration of antioxidant and antibacterial properties, which were absent in the original pristine polymer.

1. Introduction

Plastics have played a strategic role in our economy, as well as in the development of modern society. The global production exceeds 300 million tonnes/year and consumes around 6% of oil [1], with almost 26 million tonnes/year of plastic waste generated only in Europe [2]. To accelerate the transition towards a circular and resource-efficient plastics economy, the European Union is working to tackle plastic pollution. Specific targets, including single-use plastics, plastic packaging, microplastics, bio-based, biodegradable, and compostable plastics have been highlighted by the EU's plastics strategy, as part of the circular economy action plan [2], which is one of the main building blocks of the European Green Deal, aiming at reducing wastes, compensating carbon footprint emissions, saving resources [3]. In this context, the biopolymer industry, intended as those materials deriving from alternative feedstock, namely biomass, and/or biodegradable, has emerged [1]. Bioplastics are used for an increasing variety of applications, ranging from consumer products to agriculture, electronics, automotive, and textiles, but packaging remains the largest sector, with 48% (1.07 million tonnes) of the total bioplastics market in 2022 [4]. However, the spreading of biopolymers is hindered by their high prices and restricted availability [5], while some concerns are related to their performance with respect to their fossil-based counterparts [6]. Therefore, research is focused on the overcoming of such drawbacks.

Among the competitive biodegradable polymers, poly(butylene succinate) (PBS), poly(ε-caprolactone) (PCL), and poly(lactic acid) (PLA) are largely diffused, thanks to their adequate tensile/impact and melt strength, viscosity, and gas barrier properties. They are employed for consumer goods, flexible packaging, agriculture, adhesives, and medical devices. Another promising biopolymer is poly(butylene succinate-*co*-adipate) (PBSA), a semicrystalline copolymer of PBS, with adipic acid as co-monomer with succinic acid and butanediol, all obtainable from sugar fermentation [7]. PBSA is an emerging material on account of its flexibility, and comparatively lower melting temperature than traditional or renewable polyesters (i.e. poly(ethylene terephthalate) (PET), bio-PET, PLA, etc.) that can be easily processed by

* Corresponding author.
E-mail address: laura.sisti@unibo.it (L. Sisti).
[1] these Authors contributed equally

https://doi.org/10.1016/j.nbt.2024.01.001
Received 19 December 2023; Received in revised form 17 January 2024; Accepted 18 January 2024
Available online 20 January 2024

common techniques such as blow-molding. Differently from PLA, it is a tough polymer with lower oxygen permeability and finds application in the textile field and agriculture [8].

Conversely, an effective approach to cost reduction in bioplastics involves utilizing organic fillers sourced from agro-industrial activities, such as residues from wine [9,10] or coffee production [8,11–13], apple pomace [14], orange peel flour [15], sweet potato by-products [16], lignin-based materials [17], farm dairy effluents [18], among others. This strategy not only reduces costs but also offers the additional benefit of valorizing materials that would otherwise be directed towards disposal, aligning with the principles of the circular economy [11]. Examples of exploitation of several types of wastes and/or by-products deriving from agriculture and food industry (i.e., coffee, oil, starch, etc.) are indeed reported [12,19–21]. Efforts are also focused on the recovery of valuable active agents from agro-wastes [13,22]. Among the agro-industrial waste products, orange peels represent a remarkable fraction: in 2020, the total consumption of fruit juice in Europe was estimated at 1.24 billion litres, and citrus juice in particular, whose industry generates about 50–60% of the total mass of citrus waste as peels remaining from juice extraction, is the predominant one [23].

Citrus sinensis is one of the most commonly grown fruit trees in the world, whose fruits are valued for their nutritional properties. The fruit is a hesperidium rich in bioactive compounds, including mainly essential oils, carotenoids, vitamins, and phenolic compounds. These secondary metabolites are important in vivo to protect fruits against insects and pathogens and also have beneficial effects on human health [24–26]. Both the pulp and the peel of the fruit have been used in the food [27,28] and pharmaceutical industries [26,29]. Indeed, peels contain valuable molecules, such as antioxidants [30] or sugars [31], that once extracted by different methods can be used in many applications [32,33]. Oil-derived polymers (i.e. polyethylene) have been modified by orange juice processing wastes [34], as well as biopolymers (i.e. PLA) [15] or hybrid matrices (i.e. chitosan/poly(vinyl alcohol) [35] and starch [36]. Orange peels have also been reported for the preparation of active edible bio-film through a reaction with glycerol [37].

In this paper, for the first time, bio-composites are formulated with a PBSA matrix loaded with micronized orange peels. PBSA is a compostable and tough material that can presently be obtained from renewable sources. Moreover, the derived composites have been characterized not only for their mechanical and thermal properties but also for their antibacterial and antioxidant characteristics given their possible application in the packaging industry or in the organic or integrated farming sector. The interaction with moisture by water contact angle measurement has been also carried out.

2. Experimental

2.1. Materials and reagents

The poly(butylene succinate co-adipate) (PBSA) used as matrix in this study is a commercially available BioPBSTM FD92PM from PTT MCC Biochem (Dusseldorf, Germany), with an approximate composition of $(PBS)_{0.7}$-$(PBA)_{0.3}$, density of 1.24 g/cm^3 and a MFR of 4.0 g/10 min (determined at 190 °C and 2.16 kg).

Orange peels (hereafter defined as OPL), deriving from citrus (*Citrus sinensis*) have been thermally treated for 6 h at 60 °C, to reduce the water amount, stabilize the filler and at the same time minimize the degradation of the biomolecules [38]. Subsequently, they were ball milled with a rotary milling equipment (MMS, Nonantola, Italy) for ten minutes in an allubit jar to reduce their dimension, and powders were sieved below 160 μm.

For the assessment of the antioxidant activity, 2,2-diphenyl-1-picrylhydrazyl (DPPH), 6-hydroxy-2,5,7,8-tetramethyl-chroman-2-carboxylic acid (Trolox), and ferric chloride were purchased from Sigma-Aldrich (St. Louis, MO, United States); 2,4,6-tripyridyl-s-triazine (TPTZ) was received from Tokyo Chemical Industry Co. Ltd. (Tokyo, Japan) and ferrous sulfate was obtained from Merck (Darmstadt, Germany).

For antibacterial activity determination, the Nutrient broth (NB) medium and plate count agar (PCA) were obtained from Oxoid (Milan, Italy).

2.2. Filler characterization

The OPL powder has been characterized using attenuated total reflection Fourier transform infrared (ATR-FT-IR) spectroscopy, thermogravimetric analysis (TGA), and scanning electron microscopy (SEM). In detail, ATR FT-IR analysis was conducted in the frequency range 650–4000 cm^{-1} using a PerkinElmer Spectrum One FT-IR spectrometer equipped with a Universal ATR sampling accessory. For each spectrum, 32 scans were performed with a resolution of 2 cm^{-1}. Thermal stability was assessed by thermogravimetric analysis (TGA), subjecting the sample to heating from 50 to 800 °C at 10 °C/min in a nitrogen atmosphere (40 ml/min), using a PerkinElmer TGA4000 apparatus. The morphology was investigated, after gold sputtering, by a FEI XL 20 SEM, equipped with a secondary electron detector.

To assess the polyphenol content, the Folin–Ciocalteu assay was used. Specifically, 0.5 g of OPL powder underwent extraction with 5 ml of ethanol/water (70:30, vol/vol) in glass vials using an ultrasonic bath for 120 min, followed by 15 min of vortex mixing. Subsequent to centrifugation (5 min at 2500 rpm), the supernatants were collected, and the residual OPL pellet underwent a second complete extraction under identical conditions [39]. The two resulting liquid extracts were combined, filtered, and stored at − 20 °C prior to analysis, conducted at $\lambda = 765$ nm using a UV–Vis Spectrophotometer (Varian Cary 100 bio, Dual Beam). Gallic acid served as the standard, and the concentration was expressed as milligrams of gallic acid equivalent (GAE) per gram of dry weight (DW).

The overall antioxidant activity of OPL was assessed through ferric ion reducing power (FRAP) and the DPPH assay following the methodologies outlined by Benzie et al. [40] and Floegel et al. [41], respectively. In the FRAP assay, 20 μl of the previously extracted liquid from OPL was combined with 60 μl of the FRAP working solution, produced by mixing a 10:1:1 solution of 0.3 M acetate buffer, 10 mM TPTZ solution in 40 mM HCl, and 20 mM ferric chloride. Following a 60-minute incubation in dark conditions, the absorbance at 593 nm was measured. The FRAP antioxidant activity was quantified in mmol Fe^{2+}/g of DW, and values were compared against a standard curve of ferrous sulfate. For the DPPH assay, 25 μl of the extracted liquid and 25 μl of H_2O were mixed with 3.45 ml of DPPH 100 μM. After a 30-minute incubation at room temperature in the dark, the reduction in absorbance at 517 nm was measured. DPPH antioxidant activity was expressed as mmol Trolox/g of DW. Values obtained from the FRAP and DPPH assays were presented as mean ± SD, with each sample analyzed in triplicate.

2.3. Bio-composites compounding and film production

The compounding procedure was conducted using a Brabender PL-2000 Plasti-Corder at 130 °C and 100 rpm for a duration of 3 min. PBSA with OPL (at concentrations of 10%, 15%, and 20% by weight relative to the polymer) were blended without any additional additives. Prior to compounding, all materials underwent a 12-hour storage period under vacuum at 60 °C to eliminate absorbed moisture. Subsequently, the batches were milled at low temperature to produce a powder, which was then applied to form films. These films, measuring approximately 10 × 10 cm with a thickness of 200 ± 30 μm, were obtained through compression molding for 65 s at 125 °C under a pressure of 550 bar, utilizing Carver equipment.

Table 1 summarizes batch compositions and labeling.

Table 1
Compositions and codes of the investigated samples.

Sample	PBSA (wt%)	OPL (wt%)
PBSA	100	0
PBSA + 10% OPL	90	10
PBSA + 15% OPL	85	15
PBSA + 20% OPL	80	20

2.4. Bio-composites characterization

2.4.1. Thermochemical, mechanical morphological and wettability analysis

All composite samples underwent characterization through both differential scanning calorimetry (DSC) using a PerkinElmer Pyris DSC6 and thermogravimetric analysis (TGA) with a PerkinElmer TGA7, under a dry nitrogen flux, utilizing approximately 10 mg of the sample. The DSC analysis was conducted in a scanning mode with three distinct scans: the initial scan ranged from 20 to 160 °C at 15 °C/min to eliminate the thermal and mechanical history of the sample, the second scan covered from 160 °C to − 70 °C, and the final scan ranged from − 70 °C to 160 °C, both at a rate of 10 °C/min.

During the cooling scan, the temperature of crystallization (T_c) and the enthalpy of crystallization (ΔH_c) were measured. The glass transition temperature (T_g), melting temperature (T_m), and the enthalpy of fusion (ΔH_m) were determined during the second heating scan. T_g was identified as the midpoint of the heat capacity increment associated with the glass-to-rubber transition. The degree of crystallinity was calculated according to Eq. (1):

$$Xc(\%) = \frac{\Delta H_m}{\Delta H_m^{\circ} \times f_w} \times 100 \quad (1)$$

where ΔH_m is the enthalpy derived from the thermograms, ΔH°_m is the melting enthalpy of the completely crystalline material (116.9 J/g) [42] and f_w is the weight fraction of polymer in the sample.

Prior to TGA tests, the samples underwent pre-treatment at 60 °C for 24 h to eliminate moisture. Subsequently, they were subjected to heating from 30 to 800 °C at a scan rate of 10 °C/min. Parameters such as onset temperatures, residues, and temperatures corresponding to the maximum degradation rates were then determined.

Surface wettability was determined by measuring the water contact angle values using a DSA-30 Krüss. For every measurement point, the average value of contact angles measured on five/six locations on the sample was taken.

The tensile test was carried out through an INSTRON 5966 machine, equipped with a 10 kN load cell (test speed 10 mm/min, temperature 19 ± 1 °C and 70 ± 10% R.H.). From each film composition, five samples were subjected to testing. Each specimen possessed an initial length of 6 cm, a width of 0.5 cm, and an average thickness of 200 ± 20 μm.

Morphological evaluation was conducted by SEM characterization on fractured film samples after gold sputtering, using a FEI XL 20 SEM, equipped with a secondary electron detector.

2.4.2. Evaluation of UV ageing

UV degradation experiments were conducted by subjecting samples (with dimensions of length 70 mm and width 5 mm) to accelerated UV degradation in air. This was achieved using a closed chamber equipped with an Osram ultra-vitalux UV-A 300 W 230 V E27 model, emitting wavelengths higher than 300 nm, for a duration of 100 h. It's worth noting that one hour of accelerated aging corresponds to 10 h of natural solar exposure. Throughout the experiments, the internal temperature was maintained at 30 ± 3 °C.

Chemical changes in the sample films were analyzed via FT-IR spectroscopy using a PerkinElmer Spectrum One instrument in attenuated total reflection mode, following various UV exposure times. Each spectrum resulted from 32 co-added scan collections at a resolution of 2 cm^{-1}. Approximately three replicates were performed for each sample, and the curves were subsequently superimposed, positioned on a common scale, and averaged using the Omnic Software.

The primary by-products arising from oxidation were identified as carbonylated and hydroxylated species, absorbing at approximately 1710 and 3500 cm^{-1}, respectively. Consequently, the hydroxyl index was calculated as the ratio between the absorbance area at 3400 cm^{-1} (A_{OH}) corresponding to hydroxyl groups and the absorbance area of the methylene groups at 2900 cm^{-1} (A_{CH2}), serving as a reference band (A_{OH}/A_{CH2} at $t \neq 0$ h in relation to A_{OH}/A_{CH2} at time $t = 0$ h).

Finally, SEM characterization was performed by a FEI XL 20 SEM, equipped with a secondary electron detector analysis on the degraded films, after gold sputtering, to evaluate the morphology of the sample after the UV treatment.

2.4.3. Determination of antibacterial activity of the bio-composites

The antibacterial activity was determined by assessing the survival of bacterial cells following contact with the samples. *Staphylococcus aureus* ATCC 6538 and *Escherichia coli* ATCC 8739 served as the target strains. The bacterial strains were cultivated aerobically in NB medium for 16 h at 37 °C, centrifuged at 7000 rpm for 10 min, washed in sterile phosphate-buffered saline, and then resuspended in the same buffer to achieve a cell suspension of approximately 10^5 colony forming units (CFU)/ml.

Subsequently, three segments of each film, each with a surface area of 2.5 cm^2, were transferred into 2 ml tubes containing 1.5 ml of the cell suspension. These tubes were gently shaken at 23 ± 1 °C and 50 rpm for a duration of 24 h. Following the incubation period, each sample was diluted at a ratio of 1:10, and the dilutions were plated on PCA. The plates were then incubated at 37 °C for 24 h under aerobic conditions. After incubation, the colonies corresponding to the viable cell count were enumerated, and the results were expressed as CFU/ml. Each analysis was conducted in triplicate.

The reduction in the number of cells upon contact with the specimen was assessed using a modification of the equation (Eq. 2) proposed by Lala et al. [43].

$$R\% = \frac{(B - A)}{B} \times 100 \quad (2)$$

where R% is the percentage of cell mortality rate, A is the average number of viable bacterial cells obtained after a 24 h exposure to the specimen, and B is the average number of viable bacterial cells after 24 h of incubation without any specimen. Statistical analyses were performed utilizing STATISTICA software (version 10). A one-way analysis of variance (ANOVA) was conducted, with a significance threshold set at $p \leq 0.05$. The HSD Tukey test was employed to determine homogeneous groups.

3. Results and discussion

3.1. Orange peel characterization

In general, orange peel contains carbohydrates such as cellulose, pectins, lignin and hemicellulose whose characteristic bands are visible by ATR FT-IR (Fig. 1) [31,44,45]. The broad, intense, absorption peaks around 3309 cm^{-1} denote a strong presence of O-H groups, resulting from the stretching vibration of hydroxyls characteristic of carbohydrates and lignin [46]. The basic structure of the lignocellulosic material can be observed through the bands at 2922 cm^{-1} and 2853 cm^{-1}, due to the symmetrical and asymmetrical stretching of C-H, and the bending vibrations around 1423 cm^{-1}, due to the aliphatic chains (CH_2 and CH_3) [47]. The signal at 1734 cm^{-1} can be assigned to carbonyl-ester groups, the peak around 1606 cm^{-1} is due to the C=C stretching ascribable to aromatic compounds [48] from lignin, while the band at 1011 cm^{-1} can be explained by the presence of C-O or C-O-C stretching vibration [49].

Fig. 2 shows the morphology of the obtained OPL powder after

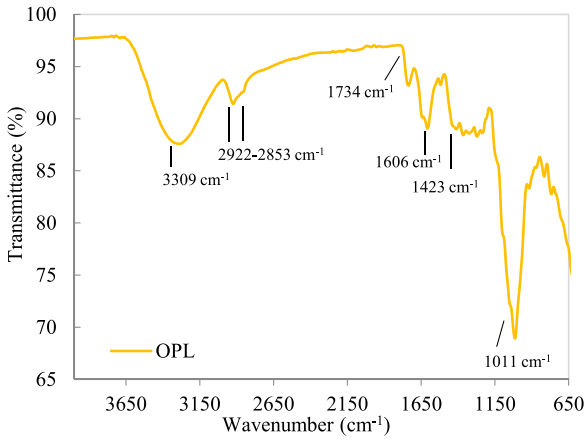

Fig. 1. : ATR FT-IR profile of OPL powder.

milling: a large distribution of size with an irregular shape and a large surface area is visible. The observed dimensions range from around 10 μm to 160 μm.

The thermal behaviour of OPL was evaluated by TGA by subjecting the sample to a preliminary isothermal heating at 80 °C for 2 min (not shown).

The thermogram, reported in Fig. 3, shows a first weight loss below 180 °C, corresponding to the removal of moisture and some lightweight molecules, which are strongly bound to OPL particles through surface tension forces and unable to be removed by the preliminary heating treatment [50].

As a matter of fact, the degradation of peels can be divided into four regions: drying (30–120 °C), low volatile loss (120–200 °C), main pyrolysis (200–400 °C), and char (400–800 °C). The significant mass loss is due to decarboxylation and decarbonylation processes, corresponding to the decomposition of hemicellulose and cellulose. Typically, the first main DTG peak corresponds to the decomposition of hemicellulose (200–240 °C), while the second one (220–400 °C) can be attributed to the decomposition of cellulose. In this region, the loss of secondary compounds contained in orange peels such as pectin, sugars and relatively low lignin takes place [51]. The last region, beyond 400 °C, corresponds to the decomposition of lignin and other more thermally stable compounds, which convert gradually to char. The final residue (23.4 wt %), produced at 800 °C, corresponds to the inorganic content of OPL and char [52,53].

To investigate the use of OPL as an active filler in polymer composites, its antioxidant activity was investigated. As already mentioned, citrus possesses several bioactive components in particular phenolic compounds, limonoids, and flavonoids [54], the amount of which depends on the plant growth conditions and fruit harvesting. Typical phenolic compounds found in the citrus peel are narirutin and naringin [54].

The polyphenol content of the orange peels found in the present study was 765.52 ± 45.96 mg GAE/100 g extract; results are in agreement with Czech et al. [55] who evaluated different citrus fruits, in particular the content of different phenolic compounds. Polyphenols are secondary metabolites that can be produced at high levels by plants, especially under stress conditions. The primary function of these bioactive compounds is to protect against UV rays, repel pathogens and regulate the plant physiological state [56]. The antioxidant activity of phenolic compounds varies depending on their molecular structure [57].

The antioxidant activity using FRAP assay was 6.19 ± 0.12 mmol Fe/100 g DW. The DPPH assay showed a percentage of discoloration of 67.25 ± 10.24% equal to 14.66 ± 2.21 μmol Trolox/g DW. Antioxidant activity was consistent with other authors evaluating antioxidant activity on the same matrix, starting from the first determination of Bocco et al. [58], till more recent data of Sir Elkhatim et al. [59]. FRAP is considered one of the most useful tests for the determination of antioxidant activity in orange peels and its value is directly associated with the polyphenols present and the activity of endogenous cellulolytic enzymes that help polyphenol extraction [60].

The antioxidant activity of oranges, and fruit in general, is an important parameter in the determination of nutritional value [61].

3.2. *Wettability and thermo-chemical characterization of bio-composites*

The bio-composites of PBSA have been processed by melt blending with 10–15-20 wt% of OPL, according to other studies carried out, highlighting the amount of 20 wt% as the threshold for the preservation of the bioactivity, possibly because of the presence of compounds that could somehow inhibit the bioactivity [11], moreover a high amount of filler generally induces brittleness in the final material.

The infrared absorption spectra of the produced samples were

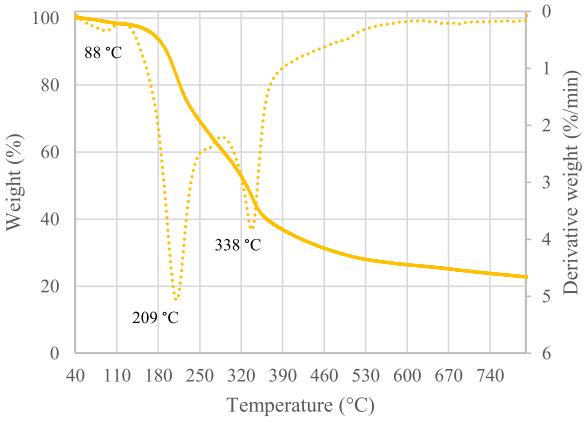

Fig. 3. : TGA and DTG profiles of OPL in nitrogen flow.

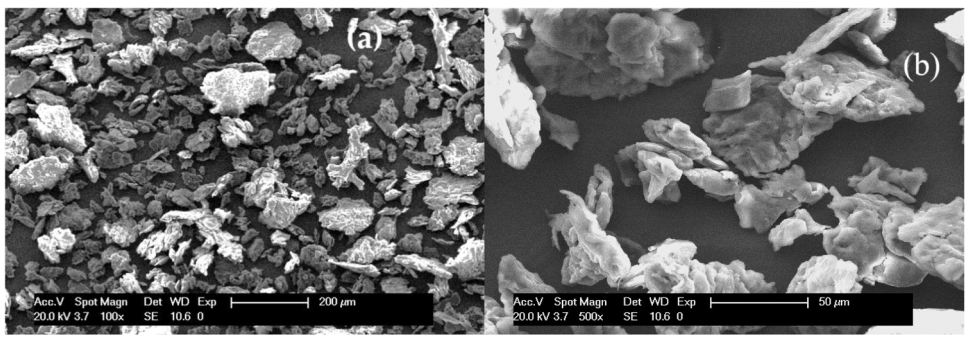

Fig. 2. : Morphology of OPL powder at (a) magnification 100 x and (b) magnification 500 x.

collected and shown in Fig. 4 in correlation with the spectrum of OPL and pristine PBSA. As analyzed above, orange peel consists mainly of cellulose, hemicellulose, lignin, and minimally of pectins and other organic compounds. The characteristic peaks of PBSA can be seen around 3400, 2990, 1715 and 1150 cm^{-1}, corresponding to O-H, C-H, C═O and O-C-C stretching, respectively. The peak around 930 cm^{-1} can be related to the bending mode of the carbonyl group [14]. The spectrum in the zoom region shows the absorptions in the range between 3750 and 2650 cm^{-1}: the filler presents the typical signal of O-H stretching mostly due to polysaccharides (from cellulose and hemicellulose) near 3309 cm^{-1} and the C-H stretching at 2922 cm^{-1}. By checking the relative intensities of the absorptions, there is an increase in OH band as a function of the increasing percentage of orange peel within the matrix (Fig. 4**b**).

Table 2 shows the thermal properties of the investigated materials. The orange peel slightly and progressively decreases the crystallization temperatures although the crystallization enthalpy remains almost unchanged, as well as the glass transition and melting temperatures. A slight decrease in the crystalline fraction is present. This allows to conclude that the filler is not acting as a nucleating agent but slightly hinders the formation of the ordered domains.

The data obtained from thermogravimetric analysis of the neat polymer and blends are reported in Table 3, while their thermograms and DTG are shown in Fig. 5.

A progressive lowering of both the initial degradation temperature and the maximum degradation temperature can be seen as the amount of filler within the matrix increases. There is also a progressive increase in strongly bound water, associated with the loss of weight, albeit minimal, that can be seen in the thermogram in the range between 150 and 250 °C.

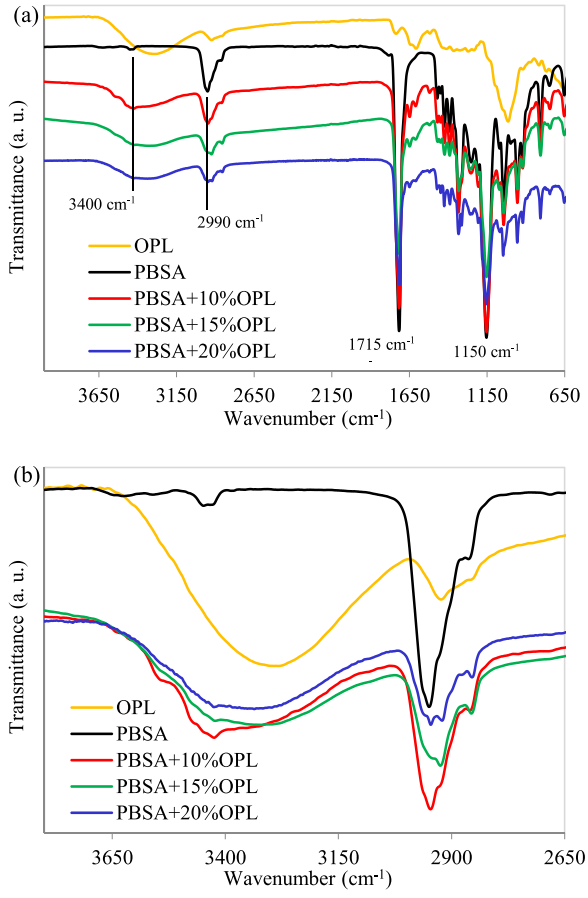

Fig. 4. : ATR FT-IR absorbance spectra of (a) OPL, PBSA and different composite samples. (b) zoom region 3800–2650 cm^{-1}.

Table 2
DSC characterization of OPL bio-composites.

. Sample	T_c (°C)	ΔH_c (J/g)	T_g (°C)	T_m (°C)	ΔH_m (J/g)	Xc (%)
PBSA	51	36	-46	85	35	29.9
PBSA + 10% OPL	50	30	-46	85	28	26.6
PBSA + 15% OPL	49	27	-45	85	27	27.2
PBSA + 20% OPL	46	25	-44	84	23	24.6

Table 3
TGA data of composite samples. Onset temperature (T_{ONSET}), maximum degradation temperature (T_{PEAK}), degradation temperature corresponding to 5% of weight loss (T_{D5}) and % remaining at the end of degradation (Residue).

Sample	T_{ONSET} (°C)	T_{PEAK} (°C)	T_{D5} (°C)	Residue (%)
PBSA	381	411	362	0.6
PBSA + 10% OPL	379	405	328	3.9
PBSA + 15% OPL	376	404	285	5.6
PBSA + 20% OPL	373	402	251	6.1

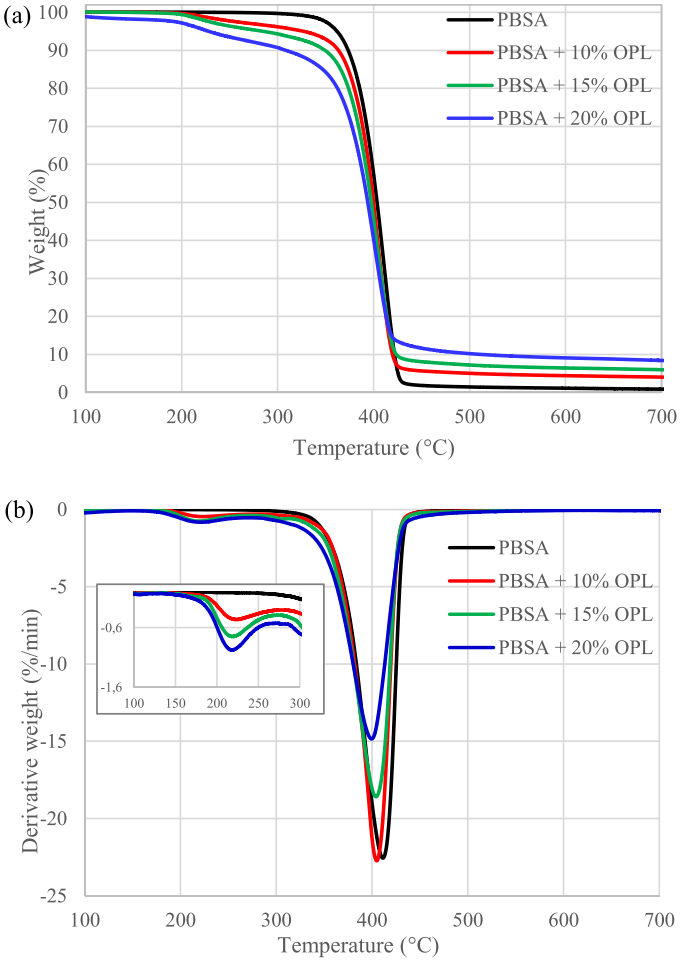

Fig. 5. : (a) TGA and (b) DTG curves of PBSA and the bio-composites.

The contact angle values are shown in Fig. 6, as a function of the amount of OPL. As a matter of fact, surface wettability is a parameter of fundamental importance because it is related to the breathability and biodegradability of materials. As can be seen, there is a decrease in contact angle with increasing quantity of peel up to 15 wt%, while from

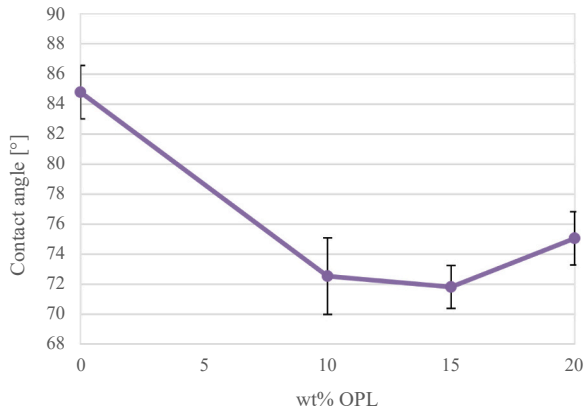

Fig. 6. : Contact angle versus the amount of OPL in bio-composites.

20 wt%, the value slightly increases. The increase in the value of the contact angle in the presence of the higher peel content could be attributable to the higher amount of hydrophobic component competing with the hydrophilic one. However, the standard deviation values are rather high, showing a certain inhomogeneity of the surface. This behaviour aligns with similar systems reported in the literature [35].

Table 4 shows the results of the mechanical characterization. The filler addition gradually increases the elastic modulus of the composites but a decreasing trend, as found in other composites [8], is found for the tensile strength. This last effect can indicate a scanty interaction between filler and matrix. As to what concerns the deformation at the maximum tensile strength and at break, a more complex behaviour seems present. A limited decrease (< 20 wt%) is found at 10 and 20 wt% OPL content but a maximum (about 20 wt%) takes place at 15 wt% OPL. Two effects seem to be acting in the composites: the one previously described, leading to more brittle behaviour and a plasticizing one possibly deriving from the diffusion of oils from the filler to the matrix. An improvement in tensile resistance could be obtained by increasing the interaction between the two phases by the use of compatibilizers as found elsewhere [14,15]. However, it should be underlined that small discrepancies could also be due to the intrinsic inhomogeneity of a natural filler, but, even at the highest OPL amount, the deformation at break is higher than the one usually reported for example for PLA [12]. In Fig. 7 the SEM pictures of the fractured surface of the bio-composite containing 20 wt% of OPL are shown as representative for all bio-composite samples. As can be seen the filler, even at the highest concentration, seems well dispersed and no clusters are detected. An imperfect interaction between the two phases is however evident from Fig. 7b.

To investigate the antioxidant effect of orange peel and, consequently, the durability of the polymer composites, the samples were subjected to accelerated photo-ageing with a UV lamp. According to the literature, the photooxidation mechanism of PBSA is similar to that of PBS, and proceeds through the: i) oxidation of the alcoholic end-groups, with formation of oligomers with carboxyl chain ends, ii) hydrogen elimination on the backbone, with subsequent hydroperoxide formation, iii) chain cleavage reaction (Norrish I), with generation of specific oxidation products [62]. The curves in Fig. 8 were obtained by periodically acquiring FTIR-ATR spectra during the ageing experiment and plotting the hydroxyl index, which can be quantitatively correlated with the amount of oxidation [20]. Due to the high content of naturally occurring ester groups in PBSA indeed, the hydroxyl band is considered more reliable as a diagnostic tool to investigate the formation of photooxidation products with respect to the carbonyl index.

As can be seen from the graph, pure PBSA shows an initial increase in the hydroxyl index, which then proceeds linearly until it undergoes a rapid acceleration after 90 h of exposure. Right from the start, a significant difference is clear between the latter and the samples, which maintain very low values between 1 and 2 throughout the evaluated time interval, in accordance with previous studies [63]. No significant differences are highlighted among the bio-composites concerning the filler amount, however, the protective role of the filler upon the matrix is clear.

The slight oscillating trends could be due to the instability of the alcoholic end-groups and their photooxidation mechanism, which leads to the formation of additional oxidation products [62].

The morphology of the surfaces submitted to UV irradiation after 100 h is reported in Fig. 9 at the same magnification. The unloaded matrix of PBSA shows the beginning of an erosion process linked to the degradation taking place, while in all the composites a similar quite smooth surface is disclosed. The observation supports the results of IR analysis.

3.3. *Antibacterial activity of bio-composites*

The antibacterial activity of biofilms is important considering their potential application in different industrial sectors such as organic or integrated farming as mulching films and food packaging to counteract potential pathogens. Antibacterial tests on the novel bio-composite films were measured evaluating cell mortality after incubation of the specimens with a suspension of two target strains: the Gram-positive *S. aureus* ATCC 6538 strain and the Gram-negative *E. coli* ATCC 8739 strain. Earlier investigations have demonstrated the substantial antimicrobial activity of orange peel extracts against various food-borne pathogens, including the strains examined in the current study [64]. However, there is a lack of studies on films incorporating this extract as a filler.

The antibacterial results are presented in Table 5 showing a significant antibacterial activity towards *S. aureus* and *E. coli* in all films containing orange peels. Regarding the Gram-positive *S. aureus* strain, a significant cell mortality was demonstrated, in the range 92–94%, compared to the control without orange peels. Cell mortality was shown to be higher in *E. coli* than in *S. aureus*, namely within the range 96–99%, possibly because of an easiest access of the antimicrobial components inside the Gram-negative cell due to the thinner peptidoglycan layer. A higher antimicrobial activity of orange peel extracts against Gram-negative strains has been shown by other authors [65]. Moreover, the percentage of mortality of *E. coli* with PBSA + 10% OPL and PBSA + 15% OPL is significantly higher than with PBSA + 20% OPL, although the difference is quantitatively low (less than 4%). This contradictory result might be due to the filler poorer dispersion within the matrix at the highest concentration, which may compromise the availability of the potential antimicrobial agents in the matrix making them not available to the bacterial cells.

As a matter of fact, the antimicrobial activity against gram-positive and gram-negative bacteria depends on the content of the phenolic compounds present in *Citrus* peels [66], with different mechanisms of action, according to Selahvarzi et al. [67]. Several findings indicate that the interactions between phenolic compounds (such as rutin, quercetin, and naringenin) and bacterial cells can lead to increased permeability of cell membranes, reduced ATP production, compromised activities of metabolic enzymes, and disruption of membrane integrity [54].

Regarding the agriculture sector, pathogenic bacteria in the agro-environmental ecosystem can be a problem for fresh product consumption. Since most of the edible parts of vegetable crops are in contact with the soil, there is a potential risk of contamination from soil

Table 4
Mechanical properties of PBSA and the bio-composites.

Sample	E (MPa)	σ_{max} (MPa)	ε_{max} (%)	ε_{break} (%)
PBSA	283.2 ± 21.1	14.1 ± 1.0	9.9 ± 0.7	13.6 ± 2.7
PBSA + 10% OPL	343.5 ± 31.7	12.1 ± 1.3	8.7 ± 1.2	12.1 ± 3.3
PBSA + 15% OPL	402.1 ± 24.4	11.3 ± 0.5	12.3 ± 4.2	16.5 ± 4.3
PBSA + 20% OPL	433.3 ± 17.5	9.1 ± 1.1	8.8 ± 1.1	10.6 ± 3.4

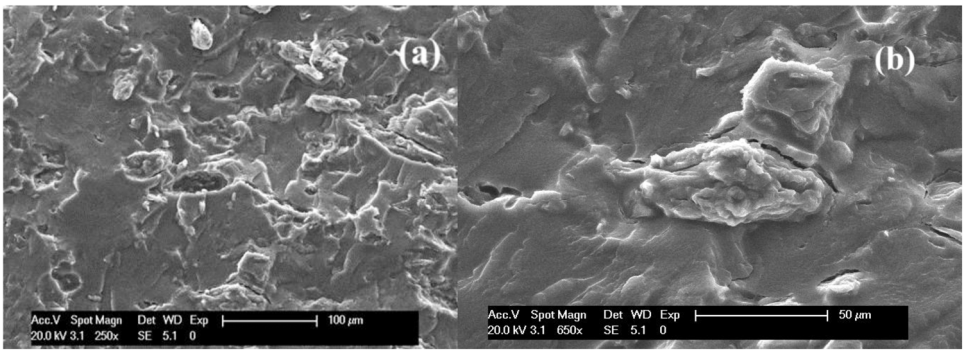

Fig. 7. : Morphology of PBSA + 20% OPL bio-composite at (a) magnification 250 x and (b) 650 x.

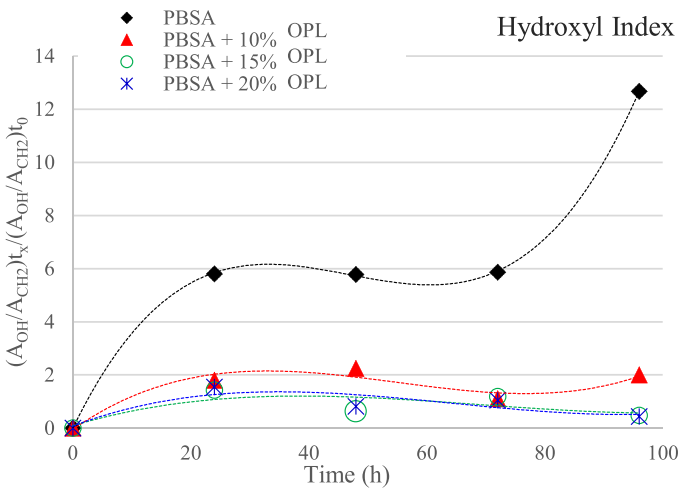

Fig. 8. : Kinetic curves of hydroxylated by-products from photooxidation of PBSA and bio-composites.

pathogens [68]. Moreover, pathogens can be taken up by the root system of crops and thus affect the quality for consumers [69]. In particular, *E. coli* can be present at high concentrations in many surface waters used for irrigation in agriculture and is one of the main indicators of irrigation water quality [70]. Therefore, antibacterial mulching films can be useful in those farming systems, such as organic or integrated farming, where chemical antimicrobial agents cannot be used to counteract pathogens. Moreover, within the food packaging industry, the presence of microbial

Table 5
Cell mortality % of PBSA and bio-composites, calculated as the average of 3 replicate tests.

Sample	Cell mortality (%) vs. *S. aureus*	Cell mortality (%) vs. *E. coli*
PBSA	0^{b}	0^{c}
PBSA + 10% OPL	93.62 ± 1.49^{a}	99.20 ± 0.12^{a}
PBSA + 15% OPL	94.12 ± 2.81^{a}	99.34 ± 0.07^{a}
PBSA + 20% OPL	92.80 ± 2.31^{a}	95.94 ± 0.53^{b}
Significance	***	***

(a,b,c) Different letters indicate significant difference (HSD Tukey's test. *** Effect significant at $p \leq 0.001$.)

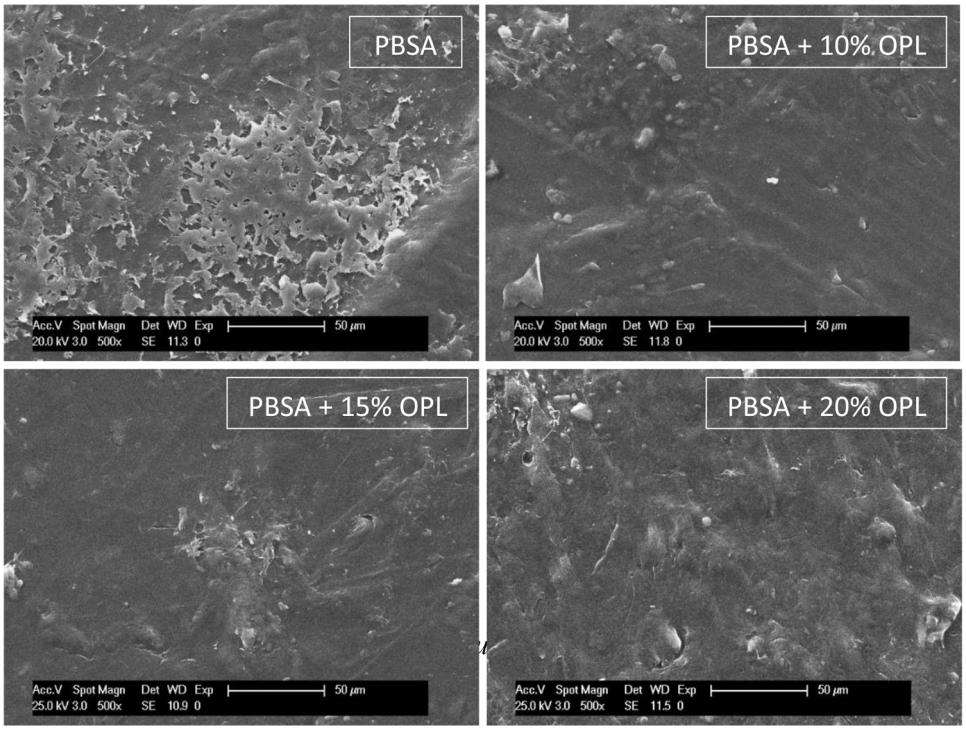

Fig. 9. : Morphology of the exposed surfaces of PBSA and bio-composites.

pathogens raises significant concerns. Hence, incorporating antimicrobial agents into the production of barrier-enhanced or active packaging materials emerges as an appealing option. This approach serves to safeguard food against the development and dissemination of microorganisms, ensuring both the quality and safety of the food products. Indeed, *S. aureus* and *E. coli* strains can contaminate fresh fruit and vegetables during storage and can cause potential foodborne outbreaks [71].

4. Conclusions

Fully biobased composites have been successfully prepared by melt compounding a bio-polyester, poly(butylene succinate-*co*-adipate) (PBSA), enriched with 10–15-20 wt% of orange peels, a food waste largely available, rich in secondary metabolites such as phenolic compounds. The addition of orange peel waste does not affect significantly the thermal stability, while a slight and progressive decrease of the crystallization temperatures and crystalline fraction within the composites is present. Concerning the mechanical properties, the results highlight a general decrease in the tensile strength, while the elongation at break remains almost constant. On the other hand, the durability of composites, as well as their antibacterial properties, are consistently higher with respect to the pristine polymer. Thus, the current strategy allows to obtain functional biobased materials, potentially useful in organic/integrated farming and in the packaging industry. Moreover, the strategy is also cost-effective, since lower amount of bioplastic can be used, and an agro-waste is fully valorized, in a virtuous example of circular economy, thus contributing to the implementation of bioplastic market, still representing only 1–2% of the global plastic market.

Funding

Authors wish to acknowledge Ecosister - “Ecosystem for Sustainable Transition in Emilia-Romagna”, project funded under the National Recovery and Resilience Plan (NRRP), Mission 04 Component 2 Investment 1.5 – NextGenerationEU, Call for tender n. 3277 dated 30/12/2021, Award Number: 0001052 dated 23/06/2022.

CRediT authorship contribution statement

Minichiello Carmen: Writing – original draft, Investigation, Formal analysis, Data curation. **Sisti Laura:** Writing – review & editing, Visualization, Validation, Supervision, Resources, Project administration, Methodology, Funding acquisition, Formal analysis, Conceptualization. **Pagliarini Elia:** Writing – original draft, Investigation, Formal analysis, Data curation. **Baffoni Loredana:** Validation, Supervision. **Di Gioia Diana:** Writing – review & editing, Visualization, Validation, Supervision, Formal analysis, Conceptualization. **Totaro Grazia:** Writing – review & editing. **Saccani Andrea:** Writing – review & editing, Visualization, Validation, Supervision, Resources, Formal analysis, Conceptualization.

Declaration of Competing Interest

The authors declare the following financial interests/personal relationships which may be considered as potential competing interests: Laura Sisti reports financial support was provided by National Recovery and Resilience Plan (NRRP), NextGenerationEU. If there are other authors, they declare that they have no known competing financial interests or personal relationships that could have appeared to influence the work reported in this paper.

References

[1] Payne J, McKeown P, Jones MD. A circular economy approach to plastic waste. Polym Degrad Stab 2019;165:170–81. https://doi.org/10.1016/j.polymdegradstab.2019.05.014.
[2] ⟨https://environment.ec.europa.eu/topics/plastics_en⟩.
[3] ⟨https://commission.europa.eu/strategy-and-policy/priorities-2019–2024/european-green-deal_en⟩.
[4] ⟨https://www.european-bioplastics.org/market/⟩.
[5] Notaro S, Lovera E, Paletto A. Consumers’ preferences for bioplastic products: a discrete choice experiment with a focus on purchase drivers. J Clean Prod 2022;330:129870. https://doi.org/10.1016/j.jclepro.2021.129870.
[6] Lettner M, Schöggl JP, Stern T. Factors influencing the market diffusion of bio-based plastics: results of four comparative scenario analyses. J Clean Prod 2017;157:289–98. https://doi.org/10.1016/j.jclepro.2017.04.077.
[7] Rosato A, Romano A, Totaro G, Celli A, Fava F, Zanaroli G, Sisti L. Enzymatic degradation of the most common aliphatic bio-polyesters and evaluation of the mechanisms involved: an extended study. Polymers 2022;14(9):1850. https://doi.org/10.3390/polym14091850.
[8] Pagliarini E, Totaro G, Saccani A, Gaggìa F, Lancellotti I, Di Gioia D, Sisti L. Valorization of coffee wastes as plant growth promoter in mulching film production: a contribution to a circular economy. Sci Total Environ 2023;871:162093. https://doi.org/10.1016/j.scitotenv.2023.162093.
[9] Saccani A, Sisti L, Manzi S, Fiorini M. PLA composites formulated recycling residuals of the winery industry. Polym Compos 2019;40(4):1378–83. https://doi.org/10.1002/pc.24870.
[10] David G, Vannini M, Sisti L, Marchese P, Celli A, Gontard N, Angellier-Coussy H. Eco-conversion of two winery lignocellulosic wastes into fillers for biocomposites: Vine shoots and wine pomaces. Polymers 2020;12(7):1530. https://doi.org/10.3390/polym12071530.
[11] Sisti L, Totaro G, Rosato A, Bozzi Cionci N, Di Gioia D, Barbieri L, Saccani A. Durability of biopolymeric composites formulated with fillers from a by-product of coffee roasting. Polym Compos 2022;43:1485–93. https://doi.org/10.1002/pc.26468.
[12] Totaro G, Sisti L, Fiorini M, Lancellotti I, Andreola FN, Saccani A. Formulation of green particulate composites from pla and pbs matrix and wastes deriving from the coffee production. J Polym Environ 2019;27:1488–96. https://doi.org/10.1007/s10924-019-01447-6.
[13] Sisti L, Celli A, Totaro G, Cinelli P, Signori F, Lazzeri A, Bikaki M, Corvini P, Ferri M, Tassoni A, Navarini L. Monomers, materials and energy from coffee by-products: a review. Sustainability 2021;13(12):6921. https://doi.org/10.3390/su13126921.
[14] Picard MC, Rodriguez-Uribe A, Thimmanagari M, Misra M, Mohanty AK. Sustainable biocomposites from Poly(butylene succinate) and apple pomace: a study on compatibilization performance. Waste Biomass Valoriz 2020;11:3775–87. https://doi.org/10.1007/s12649-019-00591-3.
[15] Quiles-Carrillo L, Montanes N, Lagaron JM, Balart S, Torres-Giner R. On the use of acrylated epoxidized soybean oil as a reactive compatibilizer in injection molded compostable pieces consisting of polylactide filled with orange peel flour. Polym Int 2018;67:1341–51. https://doi.org/10.1002/pi.5588.
[16] Vannini M, Marchese P, Sisti L, Saccani A, Mu T, Sun H, Celli A. Integrated efforts for the valorization of sweet potato by-products within a circular economy concept: biocomposites for packaging applications close the loop. Polymers 2021;13(7):1048. https://doi.org/10.3390/polym13071048.
[17] Sisti L, Kalia S, Totaro G, Vannini M, Negroni A, Zanaroli G, Celli A. Enzymatically treated curaua fibers in poly (butylene succinate)-based biocomposites. J Environ Chem Eng 2018;6(4):4452–8. https://doi.org/10.1016/j.jece.2018.06.066.
[18] Le Guen MJ, Thoury-Monbrun V, Castellano Roldán JM, Hill SJ. Assessing the potential of farm dairy effluent as a filler in novel PLA biocomposites. J Polym Environ 2017;25:419–26. https://doi.org/10.1007/s10924-016-0824-1.
[19] Sisti L, Gioia C, Totaro G, Verstichel S, Cartabia M, Camere S, Celli A. Valorization of wheat bran agro-industrial byproduct as an upgrading filler for mycelium-based composite materials. Ind Crops Prod 2021;170:113742. https://doi.org/10.1016/j.indcrop.2021.113742.
[20] Sisti L, Totaro G, Celli A, Diouf-Lewis A, Verney V, Leroux F. A new valorization route for Olive Mill wastewater: Improvement of durability of PP and PBS composites through multifunctional hybrid systems. J Environ Chem Eng 2019;7:103026. https://doi.org/10.1016/j.jece.2019.103026.
[21] Totaro G, Sisti L, Vannini M, Marchese P, Tassoni A, Lenucci MS, Lamborghini M, Kalia S, Celli A. A new route of valorization of rice endosperm by-product: production of polymeric biocomposites. Compos Part B: Eng 2018;139:195–202. https://doi.org/10.1016/j.compositesb.2017.11.055.
[22] Grimaldi M, Pitirollo O, Ornaghi P, Corradini C, Cavazza A. Valorization of agro-industrial byproducts: Extraction and analytical characterization of valuable compounds for potential edible active packaging formulation. Food Packag Shelf Life 2022;33:100900. https://doi.org/10.1016/j.fpsl.2022.100900.
[23] Giannakis N, Carmona-Cabello M, Makri A, Leiva-Candia D, Filippi K, Argeiti C, Pateraki C, Dorado MP, Koutinas A, Stylianou E. Spent coffee grounds and orange peel residues based biorefinery for microbial oil and biodiesel conversion estimation. Renew Energy 2023;209:382–92. https://doi.org/10.1016/j.renene.2023.01.110.
[24] Seigler DS. Plant Secondary Metabolism. Springer New York, NY; 1998.
[25] Satari B, Karimi K. Citrus processing wastes: environmental impacts, recent advances, and future perspectives in total valorization. Resour, Conserv Recycl 2018;129:153–67. https://doi.org/10.1016/j.resconrec.2017.10.032.

[26] Singh B, Singh JP, Kaur A, Singh N. Phenolic composition, antioxidant potential and health benefits of citrus peel. Food Res Int 2020;132:109114. https://doi.org/10.1016/j.foodres.2020.109114.

[27] Hou J, Liang L, Wang Y. Volatile composition changes in navel orange at different growth stages by HS-SPME–GC–MS. Food Res Int 2020;136:109333. https://doi.org/10.1016/j.foodres.2020.109333.

[28] Xiang Z, Chen X, Qian C, He K, Xiao X. Determination of volatile flavors in fresh navel orange by multidimensional gas chromatography quadrupole time-of-flight mass spectrometry. Anal Lett 2020;53(4):614–26. https://doi.org/10.1080/00032719.2019.1662429.

[29] Sicari V, Loizzo MR, Romeo R, Leporini M, Tundis R, Poiana M. Addition of orange by-products (dry peel) in orange jam: evaluation of physicochemical characteristics, bioactive compounds and antioxidant activity. Med Sci Forum 2021;2(1):11. https://doi.org/10.3390/CAHD2020-08561.

[30] Gavahian M, Chu YH, Khaneghah AM. Recent advances in orange oil extraction: an opportunity for the valorization of orange peel waste a review. Int J Food Sci Technol 2019;54:925–32. https://doi.org/10.1111/ijfs.13987.

[31] Ayala JR, Montero G, Coronado MA, García C, Curiel-Alvarez MA, León JA, Sagaste CA, Montes DG. Characterization of orange peel waste and valorization to obtain reducing sugars. Molecules 2021;26:1348. https://doi.org/10.3390/molecules26051348.

[32] Siles López JÁ, Li Q, Thompson IP. Biorefinery of waste orange peel. Crit Rev Biotechnol 2010;30:63–9. https://doi.org/10.3109/07388550903425201.

[33] Mohsin A, Hussain MH, Zaman WQ, Mohsin MZ, Zhang J, Liu Z, Tian X, Salim-Ur-Rehman, Khan IM, Niazi S, Zhuang Y, Guo M. Advances in sustainable approaches utilizing orange peel waste to produce highly value-added bioproducts. Crit Rev Biotechnol 2022;42:1284–303. https://doi.org/10.1080/07388551.2021.2002805.

[34] Fehlberg J, McKay S, Matuana LM, Almenar E. Use of orange juice processing waste to produce films using blown film extrusion for food packaging. J Food Eng 2023;341:111337. https://doi.org/10.1016/j.jfoodeng.2022.111337.

[35] Terzioglu P, Güney F, Parın FN, Sen I, Tuna S. Biowaste orange peel incorporated chitosan/polyvinyl alcohol composite films for food packaging applications. Food Packag Shelf Life 2021;30:100742. https://doi.org/10.1016/j.fpsl.2021.100742.

[36] Quilez-Molina AI, Oliveira-Salmazo L, Amezúa-Arranz C, Lopez-Gil A, Rodríguez-Perez MA. Evaluation of the acid hydrolysis as pre-treatment to enhance the integration and functionality of starch composites filled with rich-in-pectin agri-food waste orange peel. Ind Crops Prod 2023;205:117407. https://doi.org/10.1016/j.indcrop.2023.117407.

[37] Karakuş E, Ayhan Z, Haskaraca G. Development and characterization of sustainable-active-edible-bio based films from orange and pomegranate peel waste for food packaging: Effects of particle size and acid/plasticizer concentrations. Food Packag Shelf Life 2023;37:101092. https://doi.org/10.1016/j.fpsl.2023.101092.

[38] Farahmandfar R, Tirgarian B, Dehghan B, Nemati A. Comparison of different drying methods on bitter orange (*Citrusaurantium L.)* peel waste: changes in physical (density and color) and essential oil (yield, composition, antioxidant and antibacterial) properties of powders. J Food Meas Charact 2020;14:862–75. https://doi.org/10.1007/s11694-019-00334-x.

[39] Del Rio D, Calani L, Dall'Asta M, Brighenti F. Polyphenolic composition of hazelnut skin. J Agric Food Chem 2011;59(18):9935–41. https://doi.org/10.1021/jf202449z.

[40] Benzie IF, Strain JJ. Ferric reducing/antioxidant power assay: direct measure of total antioxidant activity of biological fluids and modified version for simultaneous measurement of total antioxidant power and ascorbic acid concentration. Methods in enzymology. Vol. 299, Academic press; 1999. p. 15–27. https://doi.org/10.1016/s0076-6879(99)99005-5.

[41] Floegel A, Kim DO, Chung SJ, Koo SI, Chun OK. Comparison of ABTS/DPPH assays to measure antioxidant capacity in popular antioxidant-rich US foods. J Food Compos Anal 2011;24(7):1043–8. https://doi.org/10.1016/j.jfca.2011.01.008.

[42] Seggiani M, Gigante V, Cinelli P, Coltelli P, Sandroni MB, Anguillesi M, Lazzeri A I. Processing and mechanical performances of Poly(Butylene Succinate–co–Adipate) (PBSA) and raw hydrolyzed collagen (HC) thermoplastic blends. Polym Test 2019;77:105900. https://doi.org/10.1016/j.polymertesting.2019.105900.

[43] Lala NL, Ramaseshan R, Bojun L, Sundarrajan S, Barhate RS, Ying-jun L, Ramakrishna S. Fabrication of nanofibers with antimicrobial functionality used as filters: protection against bacterial contaminants. Biotechnol Bioeng 2007;97:1357–65. https://doi.org/10.1002/bit.21351.

[44] Sisti L, Totaro G, Vannini M, Fabbri P, Kalia S, Zatta A, Celli A. Evaluation of the retting process as a pre-treatment of vegetable fibers for the preparation of high-performance polymer biocomposites. Ind Crops Prod 2016;81:56–65. https://doi.org/10.1016/j.indcrop.2015.11.045.

[45] Yang H, Yan R, Chen H, Lee HD, Zheng C. Characteristics of hemicellulose, cellulose and lignin pyrolysis. Fuel 2007;86(12–13):1781–8. https://doi.org/10.1016/j.fuel.2006.12.013.

[46] Zapata B, Balmaseda J, Fregoso-Israel E, Torres-García E. Thermo-kinetics study of orange peel in air. J Therm Anal Calorim 2009;98:309–15. https://doi.org/10.1007/s10973-009-0146-9.

[47] Mckendry P. Energy production from biomass (part 1): overview of biomass. Bioresour Technol 2002;83(1):37–46. https://doi.org/10.1016/S0960-8524(01)00118-3.

[48] Demirbas A. Mechanisms of liquefaction and pyrolysis reactions of biomass. Energy Convers Manag 2000;41(6):633–46. https://doi.org/10.1016/S0196-8904(99)00130-2.

[49] Ramakuela M., Adeniyi A., Onyango M., Mbaya R., Oyewo O. Performance Evaluation of orange peels ass antiscaling agent for pretreatment of water. 11th ICARD| IMWA|MWD 2018 Conference – "Risk to Opportunity". Wolkersdorfer, Ch; Sartz, L; Weber, A; Burgess, J; Tremblay, G. (Editors).

[50] Kamsonlian S, Suresh S, Majumder CB, Chand S. Characterization of banana and orange peels: biosorption mechanism. Int J Sci Technol Manag 2011;2(4):1–7.

[51] Santos CM, Dweck J, Viotto RS, Rosa AH, De Morais LC. Application of orange peel waste in the production of solid biofuels and biosorbents. Bioresour Technol 2015;196:469–79. https://doi.org/10.1016/j.biortech.2015.07.114.

[52] Lopez-Velazquez MA, Santes V, Balmaseda J, Torres-Garcia E. Pyrolysis of orange waste: a thermo-kinetic study. J Anal Appl Pyrolysis 2013;99:170–7. https://doi.org/10.1016/j.jaap.2012.09.016.

[53] Indulekha J, Gokul Siddarth MS, Kalaichelvi P, Arunagiri A. Characterization of citrus peels for bioethanol production. Materials, Energy and Environment Engineering: Select Proceedings of ICACE 2015. Singapore: Springer; 2017. p. 3–12. https://doi.org/10.1007/978-981-10-2675-1_1.

[54] Shehata MG, Awad TS, Asker D, El Sohaimy SA, Abd El-Aziz NM, Youssef MM. Antioxidant and antimicrobial activities and UPLC-ESI-MS/MS polyphenolic profile of sweet orange peel extracts. Curr Res Food Sci 2021;4:326–35. https://doi.org/10.1016/j.crfs.2021.05.001.

[55] Czech A, Malik A, Sosnowska B, Domaradzki P. Bioactive substances, heavy metals, and antioxidant activity in whole fruit, peel, and pulp of citrus fruits. Int J Food Sci 2021:1–14. https://doi.org/10.1155/2021/6662259.

[56] Babenko LM, Smirnov OE, Romanenko KO, Trunova OK. Kosakivska IV. Phenolic compounds in plants: biogenesis and functions. The Ukrainian. Biochem J 2019;91(3):5–18. https://doi.org/10.15407/ubj91.03.00.

[57] Maqsood S, Benjakul S. Comparative studies of four different phenolic compounds on in vitro antioxidative activity and the preventive effect on lipid oxidation of fish oil emulsion and fish mince. Food Chem 2010;119(1):123–32. https://doi.org/10.1016/j.foodchem.2009.06.004.

[58] Bocco A, Cuvelier ME, Richard H, Berset C. Antioxidant activity and phenolic composition of citrus peel and seed extracts. J Agric Food Chem 1998;46(6):2123–9. https://doi.org/10.1021/jf9709562.

[59] Sir Elkhatim KA, Elagib RAA, Hassan AB. Content of phenolic compounds and vitamin C and antioxidant activity in wasted parts of Sudanese citrus fruits. Food Sci Nutr 2018;6(5):1214–9. https://doi.org/10.1002/fsn3.660.

[60] Li BB, Smith B, Hossai MD. Extraction of phenolics from citrus peels: II. Enzyme-assisted extraction method. Sep Purif Technol 2006;48(2):189–96. https://doi.org/10.1016/j.seppur.2005.07.019.

[61] Rice-Evans CA, Miller NJ, Paganga G. Structure-antioxidant activity relationships of flavonoids and phenolic acids. Free Radic Biol Med 1996;20(7):933–56. https://doi.org/10.1016/0891-5849(95)02227-9.

[62] Carroccio S, Rizzarelli P, Puglisi C, Montaudo G. MALDI investigation of photooxidation in aliphatic polyesters: poly(butylene succinate). Macromolecules 2004;37:6576–86. https://doi.org/10.1021/ma049633e.

[63] Wang JM, Wang H, Chen EC, Chen YJ, Wu TM. Role of organically-modified Zn-Ti layered double hydroxides in poly(butylene succinate-co-adipate) composites: enhanced material properties and photodegradation protection. Polymers 2021;13:2181. https://doi.org/10.3390/polym13132181.

[64] Lawal D, Bala JA, Aliyu SY, Huguma MA. Phytochemical screening and in vitro anti-bacterial studies of the ethanolic extract of *Citrus senensis* (Linn.) peel against some clinical bacterial isolates. Int J Innov Appl Stud 2013;2(2):138–45.

[65] Casquete R, Castro SM, Martín A, Ruiz-Moyano S, Saraiva JA, Córdoba MG, Teixeira P. Evaluation of the effect of high pressure on total phenolic content, antioxidant and antimicrobial activity of citrus peels. Innov Food Sci Emerg Technol 2015;31:37–44. https://doi.org/10.1016/j.ifset.2015.07.005.

[66] Gabriele M, Frassinetti S, Caltavuturo L, Montero L, Dinelli G, Longo V, Di Gioia D, Pucci L. Citrus bergamia powder: antioxidant, antimicrobial and anti-inflammatory properties. J Funct Foods 2017;31:255–65. https://doi.org/10.1016/j.jff.2017.02.007.

[67] Selahvarzi A, Ramezan Y, Sanjabi MR, Mirsaeedghazi H, Azarikia F, Abedinia A. Investigation of antimicrobial activity of orange and pomegranate peels extracts and their use as a natural preservative in a functional beverage. J Food Meas Charact 2021;15:5683–94. https://doi.org/10.1007/s11694-021-01141-z.

[68] Nassarawa SS, Luo Z, Lu Y. Conventional and emerging techniques for detection of foodborne pathogens in horticulture crops: a leap to food safety. Food Bioprocess Technol 2022;15(6):1248–67. https://doi.org/10.1007/s11947-021-02730-y.

[69] Standing TA, Du Plessis E, Duvenage S, Korsten L. Internalisation potential of *Escherichia coli* O157:H7, *Listeria monocytogenes*, *Salmonella enterica subsp. enterica* serovar *Typhimurium* and *Staphylococcus aureus* in lettuce seedlings and mature plants. J Water Health 2013;11(2):210–23. https://doi.org/10.2166/wh.2013.164.

[70] Perulli GD, Gaggia F, Sorrenti G, Donati I, Boini A, Bresilla K, Manfrini L, Baffoni L, Di Gioia D, Corelli Grappadelli L, Spinelli F, Morandi B. Treated wastewater as irrigation source: a microbiological and chemical evaluation in apple and nectarine trees. Agric Water Manag 2021;244:106403. https://doi.org/10.1016/j.agwat.2020.106403.

[71] Wadamori Y, Gooneratne R, Hussain MA. Outbreaks and factors influencing microbiological contamination of fresh produce. J Sci Food Agric 2017;97(5):1396–403. https://doi.org/10.1002/jsfa.8125.